Intricate features of electron and hole skew scattering in semiconductors

M. A. Rakitskii,[1] K. S. Denisov,[1] E. Lähderanta,[1] and I. V. Rozhansky[1,2,*]
[1]*LUT University, FI-53851 Lappeenranta, Finland*
[2]*Department of Condensed Matter Physics, Weizmann Institute of Science, Rehovot 76100, Israel*

(Received 27 March 2022; revised 18 July 2022; accepted 18 July 2022; published 16 August 2022)

We study features of mobile carriers' skew scattering in nonmagnetic semiconductors emerging due to a combination of spin-orbit coupling in a crystal band structure and a nontrivial inner structure of impurities. In particular, we show that a nonzero magnetic moment of the impurity generally leads to the anomalous Hall effect (AHE) in the absence of the spin polarization of the mobile carriers, the effect arising from spin-independent scattering asymmetry due to exchange interaction. We analyze the skew scattering in bulk zinc-blende semiconductors for both electron and hole states and emphasize the crucial role of the impurity spin polarization for the emergent AHE for the valence band holes. We also revisit the skew scattering in quantum wells showing that the cancellation of the extrinsic contribution to the AHE common for two-dimensional systems can be lifted off depending on both the electron wave function and the impurity structure.

DOI: 10.1103/PhysRevB.106.085203

I. INTRODUCTION

A variety of spin transport phenomena constituting the core of modern spintronics are based on the spin separation, and, more generally, charge carriers' separation by their spin, valley, or pseudospin characteristic [1,2]. The transverse spin separation is important for the spin-orbit torques [3,4] and also can be combined with spin to charge conversion [5]. Naturally, the comprehensive understanding of microscopics underlying these phenomena is essential for the progress in the domain.

Skew scattering of electrons on electrically charged dopants has been long known as an extrinsic mechanism of the spin Hall effect (SHE) and anomalous Hall effect (AHE) [6,7]. It is generally accepted that it stems from the spin-orbit coupling (SOC) as described by Mott and further developed by Smith [8,9]. In the course of time it has been established that this effect is sensitive both to the microscopic mechanism of the SOC and also to the inner structure of the scatterer. For instance, in the original viewpoint of Mott scattering it is assumed that the SOC is provided by the core electric fields generated by a heavy impurity atom. It has been also shown that the role of the impurity-driven SOC can be to introduce the fine structure of the virtual bound states, i.e., the energy splittings with respect to the total angular momentum [10,11]. Consequently, the resonant scattering on the virtual bound states leads to the enhancement of the anomalous Hall effect [11,12].

Apart from the atomic structure of the charged scattering center itself, the extrinsic mechanism of the AHE can be induced by the complex structure of the electronic band states originating from the SOC in the host material [13]. When SOC affects the crystal band structure, the electron scattering on a spin-independent potential such as a Coulomb center becomes asymmetrical [14,15]. In this case the Hall response depends on the host material properties; calculations of the Hall resistivity lead to qualitatively different results strongly depending on the model of the crystal SOC. For instance, for a 2D case the skew scattering can be suppressed for the Rashba model [16,17], but not for Dirac electrons [13,18].

The physical picture of the skew scattering and AHE becomes more complicated when both an impurity has a complex inner structure and the electronic band structure is modified by SOC. To date this situation has been mostly considered for metallic systems via first-principles calculations [19–22]. A particularly interesting situation occurs when the impurity has an inner magnetic moment. The break of time-reversal symmetry required for the skew scattering can then be provided by the scatterer magnetic moment rather than by incident electron spin polarization; consequently, the AHE can emerge even for nonpolarized electrons [11,23–25].

While some discussion is going on for metallic systems [19–21], the effects of the interplay between impurity inner moment and SOC-affected band structure on the anomalous transport in semiconductors are much less investigated. In semiconductors the features of the skew scattering can be analyzed analytically in the vicinity of the Brillouin zone center (Γ point). That makes it possible to clarify the physics responsible for the modification of AHE. For metallic systems an accurate analysis of the skew scattering requires more detailed description of the band structure thus requiring DFT-based numerical approaches [19–21].

In the present paper we consider various cases of skew scattering of electrons and holes resulting from the combination of the SOC in the host nonmagnetic crystal and an inner magnetic moment of an impurity. On the basis of $\boldsymbol{k}\cdot\boldsymbol{p}$ theory for an electronic band structure we derive analytical results for the skew-scattering rates and the associated AHE conductivity covering both bulk and two-dimensional types of spectrum. We demonstrate that the properties of skew-scattering induced AHE and SHE are essentially sensitive to microscopic details of the considered material systems, as well as to the features

*rozhansky@gmail.com

of the impurities providing richer access to the microscopic physics of the effect.

The crystal band structure accounted for in our considerations also gives rise to intrinsic mechanisms of AHE and SHE [7,18], so it is worth commenting on conditions when the considered extrinsic contribution would play the dominant role in experiments. The skew scattering appears in the first order with respect to the scattering time $\sigma_H \propto \tau$, while other mechanisms of AHE, including Berry's phase, side jump, or cluster skew scattering [26], behave as $\sigma_H \propto \tau^0$ leading to different scaling laws between transversal and longitudinal resistivities for the skew scattering $\rho_H \propto \rho_{xx}$ and $\rho_H \propto \rho_{xx}^2$ for all others. Therefore, the analysis presented in this paper is valid for sufficiently clean samples [27] ($\rho_{xx}^2 \ll \rho_{xx}$) with some fraction of impurities having finite magnetic moment. One example of a nonmagnetic semiconductor where the AHE is argued to be driven by carrier skew scattering on magnetic dopants is high-mobility electron gas in ZnO-based structures [23]. Also, we focus on essentially nonmagnetic semiconductors when the small density of magnetic impurities does not lead to the spontaneous spin splitting of the band states. In this sense we expect the Berry's phase dissipationless contribution to AHE [28] to be entirely suppressed.

Various intrinsic mechanisms underlying SHE and AHE in semiconductors have been discussed for the valence band holes [28–33]. The skew scattering of the holes in III-V semiconductors in the context of the extrinsic AHE has been believed to be similar to that of the electrons. Moreover, the effect is expected to be stronger as there is no small parameter Δ/E_0 (where Δ is the spin-orbit splitting and E_0 is the band gap) controlling SOC for the conduction band electrons. However, in a dilute p-type (Ga,Mn)As magnetic semiconductor for low resistivities the transverse vs longitudinal resistance scaling is quadratic or at least considerably superlinear suggesting that the dominating mechanism of AHE can be other than the skew scattering [34–36]. In metals such scaling can be also explained by inelastic scattering of electrons on phonons and spin waves [6]. Essentially, the domination of superlinear scaling mechanisms is favored for a larger resistance assuming the system is still beyond hopping conductivity [28]. Moreover, the microscopic mechanism of the valence band holes' skew scattering in semiconductors and its difference from the electron skew scattering has not been investigated theoretically. Neither has skew scattering of holes on magnetic centers been studied so far.

The paper is organized as follows. In Sec. II we present the model framework for analysis of asymmetric scattering contribution to the AHE. In the following sections the approach is applied to the relevant cases.

II. GENERAL THEORY

We analyze skew-scattering driven contributions to the transverse electric and spin Hall currents (see Fig. 1) on the basis of the Boltzmann kinetic equation:

$$(e\boldsymbol{E}\boldsymbol{v}_s)\frac{\partial f_s^0}{\partial \varepsilon} = \mathrm{St}[\delta f_s], \tag{1}$$

where $f_s = f_s^0 + \delta f_s$ is the carrier distribution function (index s accounts for the spin states), which consists of the equilibrium f_s^0 and nonequilibrium δf_s parts, $\boldsymbol{E}$ is an applied electric field, and $\boldsymbol{v}_s = \partial\varepsilon_s/\partial\boldsymbol{p}$ is a velocity in the s subband. The collision integral can be written as

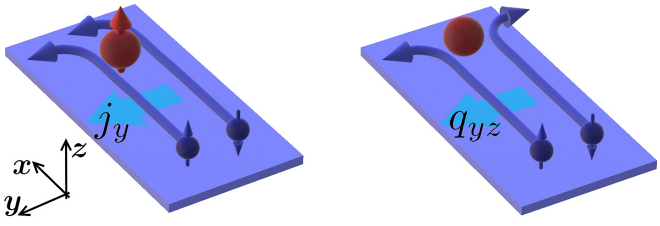

(a) (b)

FIG. 1. Illustration of spin-independent (a) and spin-dependent (b) contributions to the skew scattering leading, respectively, to charge Hall effect and spin Hall effect.

$$\mathrm{St}[\delta f_s(\boldsymbol{k})] = \frac{2\pi}{\hbar} n_i \sum_{\boldsymbol{k}'s'} \delta\left(\varepsilon_k^s - \varepsilon_{k'}^{s'}\right)\left(\left|T_{kk'}^{ss'}\right|^2 \delta f_{s'}(\boldsymbol{k}') - \left|T_{k'k}^{s's}\right|^2 \delta f_s(\boldsymbol{k})\right), \tag{2}$$

where n_i is the impurity concentration, $\varepsilon_{\boldsymbol{k}}^s$ is a particle energy in the s subband, and $T_{kk'}^{ss'}$ is the corresponding scattering T-matrix element for the scattering from the state $(\boldsymbol{k}, s)$ into the state $(\boldsymbol{k}', s')$.

The skew-scattering contributions are related to the asymmetric parts of $|T_{kk'}^{ss'}|^2$. In this paper we treat the electron scattering on an impurity characterized by a potential $\hat{V}$ perturbatively. The corresponding T matrix can be expanded in Born series

$$\hat{T} = \hat{V} + \hat{V}\hat{G}_0\hat{V} + \dots, \tag{3}$$

where $\hat{G}_0$ is the free Green's function of mobile carriers in a semiconductor. As is well known, the skew scattering does not appear in the first Born approximation so one should keep the second order in (3). The asymmetric term $W_{kk'}^{ss'}$ in $|T_{kk'}^{ss'}|^2$ takes the form [18]

$$W_{kk'}^{ss'} = 2\pi \sum_l \nu_l(\varepsilon)\left\langle \mathrm{Im}\left(V_{k'k}^{s's} V_{kq}^{sl} V_{qk'}^{ls'}\right)\right\rangle_{\Omega_q}, \tag{4}$$

where the sum is over the spin of the intermediate state, ν_l is the density of states (DOS) in l subband, and $\langle\,\rangle_{\Omega_q}$ denotes averaging over the angles of the intermediate state wave vector $\boldsymbol{q}$. Note that in some cases the third-order contribution to $W_{kk'}^{ss'}$ might vanish, so one should go in higher orders of the Born series [17,37]. In this paper we deal with systems where the third-order contribution plays the major role. In the following sections we analyze the features of $W_{kk'}^{ss'}$ for different cases and describe the related properties of the emerging Hall response.

We assume the relaxation time approximation and split the collision integral into two parts:

$$\mathrm{St}[\delta f_s(\boldsymbol{k})] = \mathrm{St}_1[\delta f_s(\boldsymbol{k})] + \mathrm{St}_2[\delta f_s(\boldsymbol{k})],$$

$$\mathrm{St}_1[\delta f_s(\boldsymbol{k})] = \frac{2\pi}{\hbar} n_i \sum_{s',\boldsymbol{k}'} \delta\left(\varepsilon_k^s - \varepsilon_{k'}^{s'}\right)\left|V_{kk'}^{ss'}\right|^2 \delta f_{s'}(\boldsymbol{k}') - \frac{\delta f_s(\boldsymbol{k})}{\tau_s},$$

$$\mathrm{St}_2[\delta f_s(\boldsymbol{k})] = \frac{2\pi}{\hbar} n_i \sum_{s',\boldsymbol{k}'} \delta\left(\varepsilon_k^s - \varepsilon_{k'}^{s'}\right) W_{kk'}^{ss'} \delta f_{s'}(\boldsymbol{k}'), \tag{5}$$

where τ_s is the quantum scattering time:

$$\frac{1}{\tau_s} = \frac{2\pi}{\hbar} n_i \sum_{s',\boldsymbol{k}'} \delta\left(\varepsilon_k^s - \varepsilon_{k'}^{s'}\right) \left|V_{k'k}^{s's}\right|^2. \tag{6}$$

The first part St_1 of the collision integral is of the second order in $\hat{V}$ and determines the longitudinal current. The second part St_2 is of the third order; it describes the scattering asymmetry leading to the transverse current. With the nonequilibrium part of the distribution function obtained from the kinetic equation the charge current is given by

$$\boldsymbol{j} = e \sum_{s,\boldsymbol{k}} \boldsymbol{v}_s f_s(\boldsymbol{k}). \tag{7}$$

In a 3D case it is convenient to expand the nonequilibrium part of the distribution function in the first spherical harmonics Y_x, Y_y, and Y_z:

$$\begin{aligned} \delta f_s(\boldsymbol{k}) &= f_x^s(k) Y_x + f_y^s(k) Y_y + f_z^s(k) Y_z, \\ Y_x &= \sqrt{\frac{3}{4\pi}} \sin\theta \cos\varphi, \quad Y_y = \sqrt{\frac{3}{4\pi}} \sin\theta \sin\varphi, \\ Y_z &= \sqrt{\frac{3}{4\pi}} \cos\theta. \end{aligned} \tag{8}$$

Higher harmonics appear to give no contribution to the transverse current. Let the external electric field $\boldsymbol{E}$ be aligned along the x axis. As will be shown below $W_{kk'}$ and $|V_{kk'}|^2$ can be represented in the following form:

$$\begin{aligned} W_{kk'}^{ss'} &= w_{ss'}(Y_x' Y_y - Y_y' Y_x), \\ \left|V_{kk'}^{ss'}\right|^2 &= \text{const.} + u_{ss'}(Y_x Y_x' + Y_y Y_y' + Y_z Y_z'), \end{aligned} \tag{9}$$

where a prime symbol denotes the spherical harmonic function dependence on (φ', θ') rather than on (φ, θ).

In the 2D case these formulas keep the same form with angular harmonics being $Y_x = \pi^{-1/2} \cos\varphi$, $Y_y = \pi^{-1/2} \sin\varphi$, $Y_z = 0$. Then the kinetic equation (1) can be rewritten in the matrix form (see Supplemental Material [48] for details),

$$eE_x \frac{\partial f^0}{\partial \varepsilon} \begin{pmatrix} V \\ 0 \end{pmatrix} = \begin{pmatrix} A & -B \\ B & A \end{pmatrix} \begin{pmatrix} F_x \\ F_y \end{pmatrix}, \tag{10}$$

where V is a vector composed of the velocities in each spin subband, F_x and F_y are vectors containing the unknown coefficients for the expansion of the nonequilibrium part of the distribution function in angular harmonics, and A and B are $n_s \times n_s$ matrices originating from the first and second parts of the collision integral, respectively (here, n_s is the number of spin subbands and ν' is the DOS in the s' subband):

$$\begin{gathered} V = \begin{pmatrix} v_1 \\ \vdots \\ v_{n_s} \end{pmatrix}, \quad F_x = \begin{pmatrix} f_x^1 \\ \vdots \\ f_x^{n_s} \end{pmatrix}, \quad F_y = \begin{pmatrix} f_y^1 \\ \vdots \\ f_y^{n_s} \end{pmatrix}, \\ A_{ss'} = \nu' u^{ss'} - \delta_{ss'} \tau_s^{-1}, \qquad B_{ss'} = \nu' w^{ss'}. \end{gathered} \tag{11}$$

Neglecting the second part of the collision integral (of the higher order in V), we find the coefficients f_x^s:

$$F_x = eE_x \frac{\partial f^0}{\partial \varepsilon} A^{-1} V. \tag{12}$$

The longitudinal conductivity is further calculated according to

$$j_x = e \sum_{s,\boldsymbol{k}} v_x^s \delta f_s. \tag{13}$$

Then, using the second part of the collision integral, the coefficients f_y^s are expressed in terms of f_x^s:

$$F_y = -A^{-1} B F_x = -eE_x \frac{\partial f^0}{\partial \varepsilon} A^{-1} B A^{-1} V. \tag{14}$$

At zero temperatures one has $(f^0)' = -\delta(\varepsilon - \varepsilon_F)$ and the transverse charge current can be calculated from

$$\begin{aligned} j_y &= e \sum_s \int \nu_s \langle v_y^s \delta f^s \rangle_\Omega d\varepsilon \\ &= e \sum_s \int \nu_s v_s f_y^s d\varepsilon = e^2 E_x \sum_s \nu_s v_s (A^{-1} B A^{-1} V)_s. \end{aligned} \tag{15}$$

One should note that the presence of asymmetric scattering does not guarantee the emergence of a charge Hall current. First, the contributions to $W_{kk'}^{ss'}$ from different spin subbands can compensate each other when substituted into the collision integral so that all the coefficients f_y^s will be equal to zero. Second, even for nonzero f_y^s, canceling can occur when the transverse current is summed over different subbands with a nonzero current in each.

III. BULK ZINC-BLENDE SEMICONDUCTORS

In this section we consider skew scattering of the mobile carriers for bulk semiconductors with zinc-blende crystal structure. Throughout our calculations we use the 14-band $\boldsymbol{k} \cdot \boldsymbol{p}$ model for GaAs-like semiconductors as shown in Fig. 2. For the electrons the $\boldsymbol{k} \cdot \boldsymbol{p}$ coupling between the Γ_6^c conductance band and $\Gamma_{7,8}^v$ valence band is essential to capture the appearance of the skew scattering. However, as will be shown below this coupling remains crucial for the skew scattering

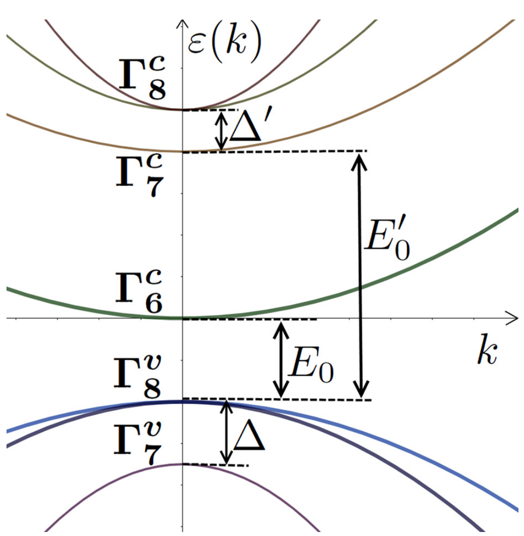

FIG. 2. Band diagram for a semiconductor with zinc-blende crystal structure.

of the valence band holes, as well as the coupling with p-like states corresponding to high-lying conduction bands $\Gamma_{7,8}^c$.

We model the scattering potential of an impurity with the following expression,

$$\hat{V} = u(\boldsymbol{r}) + \hat{u}_X(\boldsymbol{r})\boldsymbol{J}\cdot\hat{\boldsymbol{\sigma}}, \tag{16}$$

where the first scalar term describes the electrostatic potential of an impurity and the second term $\hat{u}_X$ represents exchange interaction of itinerant electrons and localized spin $\boldsymbol{J}$ of the impurity. The electron spin is described by the Pauli matrices operator. In this work we treat the impurity spin $\boldsymbol{J}$ as a fixed vector and do not account for its dynamics (though some interesting effects can arise in the Kondo regime [22]). Let us assume that a weak external magnetic field is applied to a sample to maintain impurity magnetization $\boldsymbol{J} = J\boldsymbol{e}_z$.

The T matrix includes matrix elements of both scalar and exchange parts of the scattering potential. We keep to a short-range impurity potential and describe its scalar part by a single matrix element u_0 unique for all Bloch states:

$$u_0 = \langle S|u|S\rangle = \langle X|u|X\rangle = \langle X'|u|X'\rangle, \tag{17}$$

where S, (X, Y, Z), (X', Y', Z') denote the Bloch amplitudes of the conductance band Γ_6^c, valence band $\Gamma_{7,8}^v$, and upper conductance band $\Gamma_{7,8}^c$, respectively. The matrix elements of the exchange interaction part calculated for different Bloch amplitudes are taken differently:

$$\alpha_{ex} = \langle S|u_X|S\rangle,\ \beta_{ex} = \langle X|u_X|X\rangle,\ \gamma_{ex} = \langle X'|u_X|X'\rangle; \tag{18}$$

the off-diagonal matrix elements are assumed to be zero [38].

A. Conduction band Γ_6^c

Let us describe the skew scattering of electrons in the conduction band Γ_6^c. The main effect leading to a finite skew scattering comes from the inner spin-orbit coupling responsible for the valence band splitting Δ into Γ_7^v and Γ_8^v states [14] (see Fig. 2). The electron wave function accounting for the admixture of spin-orbit split valence bands has the following form [14,39]:

$$\Psi_{\boldsymbol{k},s} = e^{i\boldsymbol{kr}}\{S + i\boldsymbol{R}[\mathcal{A}\boldsymbol{k} - i\mathcal{B}(\hat{\boldsymbol{\sigma}}\times\boldsymbol{k})]\}|\chi_s\rangle, \tag{19}$$

$$\mathcal{A} = P\frac{3E_0 + 2\Delta}{3E_0(E_0+\Delta)},\quad \mathcal{B} = -P\frac{\Delta}{3E_0(E_0+\Delta)}, \tag{20}$$

$$P = \frac{i\hbar}{m}\langle S|\hat{p}_x|X\rangle, \tag{21}$$

where S is the Bloch amplitudes for the conduction band Γ_6^c and $\boldsymbol{R} = (X, Y, Z)$ are the degenerate valence band states at the Γ point in the absence of spin-orbit splitting Γ_{15}; $|\chi_s\rangle = |\uparrow,\downarrow\rangle$ denotes the electron spin. The parameter $\mathcal{B}$ appears only due to nonzero Δ; this term is vital for the appearance of the scattering asymmetry.

The matrix element of the scattering potential given by Eq. (16) calculated between the $\Psi_{\boldsymbol{k},s}$ and $\Psi_{\boldsymbol{k}',s'}$ states is given by

$$\begin{aligned}\hat{V}_{kk'} = {}& u_0[1 + (\mathcal{A}^2 + 2\mathcal{B}^2)(\boldsymbol{k}\cdot\boldsymbol{k}') + i(2\mathcal{AB}+\mathcal{B}^2)\hat{\boldsymbol{\sigma}}\cdot(\boldsymbol{k}\times\boldsymbol{k}')] + \alpha_{ex}(\boldsymbol{J}\cdot\hat{\boldsymbol{\sigma}})\\ &+ \beta_{ex}[i(2\mathcal{AB}-\mathcal{B}^2)\boldsymbol{J}\cdot(\boldsymbol{k}\times\boldsymbol{k}') + \mathcal{A}^2(\boldsymbol{J}\cdot\hat{\boldsymbol{\sigma}})(\boldsymbol{k}\cdot\boldsymbol{k}') - \mathcal{B}^2(\boldsymbol{J}\cdot\boldsymbol{k})(\hat{\boldsymbol{\sigma}}\cdot\boldsymbol{k}') - \mathcal{B}^2(\hat{\boldsymbol{\sigma}}\cdot\boldsymbol{k})(\boldsymbol{J}\cdot\boldsymbol{k}')].\end{aligned} \tag{22}$$

Being interested in the asymmetric scattering, one should drop all the k-dependent terms from Eq. (22) which are symmetric to $\boldsymbol{k}\leftrightarrow\boldsymbol{k}'$. Indeed, the skew-scattering rate Eq. (4) is quadratic in k in the leading order so only chiral terms of the form $\boldsymbol{k}\times\boldsymbol{k}'$ should be kept.

The exchange interaction part of the scattering potential also contributes to the longitudinal conductivity [40,41]. When the impurities are spin-polarized the transport time from Eq. (6) becomes spin-dependent:

$$\frac{1}{\tau_{\uparrow,\downarrow}} = \frac{2\pi}{\hbar}n_i\nu(u_0 \pm \alpha_{ex}J)^2. \tag{23}$$

In the linear order with respect to u_X/u_0 the difference between the times is

$$\Delta\tau = \tau_\downarrow - \tau_\uparrow = \frac{4\alpha_{ex}J\tau}{u_0},\quad \frac{1}{\tau} = \frac{2\pi}{\hbar}n_i\nu u_0^2. \tag{24}$$

Substituting the expressions for the scattering times into matrix A of Eq. (11), we get for the longitudinal conductivity σ_{xx} from Eq. (13)

$$\sigma_{xx} = \sigma_{xx}^\uparrow + \sigma_{xx}^\downarrow,\quad \sigma_{xx}^s = \frac{n_0e^2\tau_s}{2m}, \tag{25}$$

where n_0 is the electron concentration. Due to the difference between spin-up and spin-down conductivity $\sigma_{xx}^\uparrow \neq \sigma_{xx}^\downarrow$ an electrical current is accompanied with the spin current q_{xz} (spin along z flows in the x direction): $q_{xz} = e^{-1}(\sigma_{xx}^\uparrow - \sigma_{xx}^\downarrow)E_x$.

We further calculate the skew-scattering rate according to Eq. (4) with the matrix elements from Eq. (22). In the leading order with respect to u_X/u_0 we obtain

$$\begin{aligned}W_{kk'}^{ss'} &= -2\pi\nu u_0^2(\boldsymbol{k}\times\boldsymbol{k}')_z(\sigma_z^{ss'}Z_0 + \delta_{ss'}Z_X),\\ Z_0 &= u_0(2\mathcal{AB}+\mathcal{B}^2),\\ Z_X &= \beta_{ex}J(2\mathcal{AB}-\mathcal{B}^2) + 2\alpha_{ex}J(2\mathcal{AB}+\mathcal{B}^2).\end{aligned} \tag{26}$$

Let us emphasize the appearance of two terms having different dependence on the electron spin state. The term related to the scalar potential contains the Pauli matrix σ_z and describes spin-dependent asymmetric scattering leading directly to the SHE. The second term with Z_X originates from the exchange interaction, being sensitive to the impurity magnetic moment rather than to the spin of the mobile electron. This type of the asymmetric scattering is spin-independent and it leads to the formation of the electric charge current even at vanishing electron spin polarization [25]. The spin-dependent contribution to the skew scattering leading to the transverse spin current and the spin-independent contributions are illustrated in Fig. 1.

The anomalous Hall conductivity can be obtained by combining τ_s and $W_{kk'}$ in Eqs. (14) and (15). The resulting expression for nonpolarized electron gas is given by

$$\sigma_{yx} = \left(P_s\theta_0 + \theta_X - \theta_0\frac{\Delta\tau}{\tau}\right)\frac{n_0 e^2\tau}{m}, \quad P_s = \frac{n_\uparrow - n_\downarrow}{n_\downarrow + n_\uparrow}, \quad (27)$$

where $\theta_{0,X} = Z_{0,X}\frac{2\pi}{3}\nu k_F^2$ have the meaning of the corresponding Hall angles, and P_s is an electron spin polarization. Note that at $P_s = 0$ there are two terms in σ_{yx}. The first one θ_X originates from the asymmetry independently of the electron spin due to the exchange scattering; the second one θ_0 results from the conversion of the transverse spin current into electrical current due to $\tau_\uparrow \neq \tau_\downarrow$.

From the experimental point of view the anomalous Hall response in a semiconductor lightly doped with magnetic impurities turns out to be a combined effect of SOC in the host material and inner structure of the magnetic impurity. Note that the admixture of the valence band is crucial for the effect. This is of no surprise for the conduction band electrons. However, as we will see further, the admixture of other bands will be also crucial for the skew scattering in the valence band, which is affected by SOC already in the zeroth order of the $\boldsymbol{k}\cdot\boldsymbol{p}$ theory.

B. Valence band

Let us now address the skew scattering of valence band holes populating the Γ_8^v band. It would be rather natural to expect that the magnitude of the skew-scattering contribution to the AHE in the Γ_8^v band would be much larger than that for the conduction band due to larger impact of SOC. However, as we demonstrate below, this argumentation fails as skew-scattering rate remains of the same order of magnitude with respect to band-structure parameters. Moreover, a magnetic moment of the scatterer becomes of key importance to have any skew scattering at all.

Let us first consider skew scattering for the valence band holes described by the Luttinger Hamiltonian in spherical approximation:

$$H = \frac{\hbar^2}{2m_0}\left[\left(\gamma_1 + \frac{5}{2}\gamma_2\right)\boldsymbol{k}^2 - 2\gamma_2(\boldsymbol{k}\cdot\hat{\boldsymbol{\mathcal{J}}})^2\right]; \quad (28)$$

here γ_1, γ_2 are Luttinger parameters, and $\hat{\boldsymbol{\mathcal{J}}}$ are the matrices of angular momentum 3/2. We use the helicity basis for the heavy-hole Ψ_{hh} and light-hole Ψ_{lh} wave functions [42]:

$$\Psi_{lh,+}(\boldsymbol{k}) = \Psi_{lh,-}(-\boldsymbol{k}) = \begin{pmatrix} -\sqrt{3}\sin\frac{\theta}{2}\cos^2\frac{\theta}{2}e^{-\frac{3i\varphi}{2}} \\ \left(3\cos^2\frac{\theta}{2} - 2\right)\cos\frac{\theta}{2}e^{-\frac{i\varphi}{2}} \\ -\left(3\sin^2\frac{\theta}{2} - 2\right)\sin\frac{\theta}{2}e^{\frac{i\varphi}{2}} \\ \sqrt{3}\sin^2\frac{\theta}{2}\cos\frac{\theta}{2}e^{\frac{3i\varphi}{2}} \end{pmatrix}, \quad (29)$$

$$\Psi_{hh,+}(\boldsymbol{k}) = \Psi_{hh,-}(-\boldsymbol{k}) = \begin{pmatrix} \cos^3\frac{\theta}{2}e^{-\frac{3i\varphi}{2}} \\ \sqrt{3}\sin\frac{\theta}{2}\cos^2\frac{\theta}{2}e^{-\frac{i\varphi}{2}} \\ \sqrt{3}\sin^2\frac{\theta}{2}\cos\frac{\theta}{2}e^{\frac{i\varphi}{2}} \\ \sin^3\frac{\theta}{2}e^{\frac{3i\varphi}{2}} \end{pmatrix}. \quad (30)$$

These wave functions are the eigenvectors of the helicity operator $\hat{\eta} = (\boldsymbol{k}/k)\cdot\hat{\boldsymbol{\mathcal{J}}}$. The notation $\pm$ stands for the positive or negative helicity, namely $\langle\Psi_{hh,\pm}|\hat{\eta}|\Psi_{hh,\pm}\rangle = \pm 3/2$ and $\langle\Psi_{lh,\pm}|\hat{\eta}|\Psi_{lh,\pm}\rangle = \pm 1/2$. In this basis the scattering times for the light holes and heavy holes entering matrix A [see Eq. (11)] are equal:

$$\tau_{lh,\pm}^{-1} = \tau_{hh,\pm}^{-1} = \frac{8\pi^2}{\hbar}n_i\langle\nu\rangle u_0^2, \quad \langle\nu\rangle = \frac{\nu_{lh} + \nu_{hh}}{2}. \quad (31)$$

The scattering asymmetry matrix B is explicitly written in the Supplemental Material [48]. We note here that the asymmetric scattering rate $W_{kk'}^{\nu\mu}$ contains multiple angular harmonics. Only the first angular harmonics with $l = 1$ are relevant for the electrical current, while higher harmonics could contribute to other physical phenomena. The rates describing skew scattering in all the scattering channels appear to have the form

$$W = \zeta\langle\nu\rangle u_0^2\beta_{ex}J(Y_x'Y_y - Y_y'Y_x), \quad (32)$$

ζ being a numerical factor, given explicitly in the Supplemental Material [48]. Note that these rates are linear in β_{ex}, so that there is no skew scattering without the exchange part of the impurity potential. Moreover, even in the presence of the exchange interaction the electric Hall current calculated by substituting A, B matrices into Eq. (15) turns out to be zero as the contributions from different channels cancel each other out.

Let us note that the skew-scattering rates generally transform when changing the wave function basis. In particular, using the basis for Γ_8^v as in Ref. [39] (rather than fixed chirality basis) we find that the matrix of asymmetry turns out to be zero $B = 0$ so the absence of AHE can be seen in this case right from the very beginning.

Since there is no skew scattering for the Luttinger Hamiltonian we further consider the Kane model and analyze whether taking into account the $\boldsymbol{k}\cdot\boldsymbol{p}$ admixture of remote bands would give rise to a finite skew scattering of the valence band holes. First, let us take into account the admixture of the Γ_6^c states of the conductance band. The heavy holes are not affected $\delta\Psi_{hh,+} = \delta\Psi_{hh,-} = 0$; for the light holes the linear in k correction to the Γ_8^v wave function appears:

$$\delta\Psi_{lh,+} = \frac{ikP}{E_0}\frac{\sqrt{6}}{3}\left(\cos\frac{\theta}{2}e^{-\frac{i\varphi}{2}}|S\uparrow\rangle + \sin\frac{\theta}{2}e^{\frac{i\varphi}{2}}|S\downarrow\rangle\right),$$

$$\delta\Psi_{lh,-} = \frac{kP}{E_0}\frac{\sqrt{6}}{3}\left(\cos\frac{\theta}{2}e^{\frac{i\varphi}{2}}|S\downarrow\rangle - \sin\frac{\theta}{2}e^{-\frac{i\varphi}{2}}|S\uparrow\rangle\right). \quad (33)$$

Using Eq. (19) one verifies $\langle\Psi_{hh,+}|\Psi_{ks}\rangle = \langle\Psi_{hh,-}|\Psi_{ks}\rangle = 0$, so the $\boldsymbol{k}\cdot\boldsymbol{p}$ coupling between the Γ_6^c and Γ_8^v bands is only via electron–light hole states. Similarly to the conduction band states considered in the previous section, the admixture of the Γ_6^c states to the light holes gives rise to the skew scattering; the corresponding asymmetric rates are given by

$$W_{lh+,lh+}^{(1)} = W_{lh+,lh-}^{(1)} = W_{lh-,lh-}^{(1)} = -\frac{2\pi^2\langle\nu\rangle kk'P^2}{9E_0^2}u_0^2(\alpha_{ex} + 10\beta_{ex})J. \quad (34)$$

We note that skew-scattering rates are nonzero only if an impurity has an inner magnetic moment. The sign of the scattering asymmetry is unique for all scattering channels within the light-hole sector as it is determined by the impurity magnetic moment.

The appearance of the same sign skew scattering is in contrast to the case of electrons from Γ_6^c; in particular it implies that the conductivity difference mechanism of the anomalous Hall resistivity driven by the scalar part of the impurity potential is suppressed for the light holes. Using Eqs. (14) and (15) we derive the following expression for the electric Hall current,

$$j_y = e^2 E_x \frac{(2m_{lh}\varepsilon_F)^3}{8\pi^5\hbar^7 n_i}\left(\frac{P}{E_0}\right)^2 \frac{(\alpha_{ex}+10\beta_{ex})J}{18\langle\nu\rangle u_0^2}. \tag{35}$$

Interestingly, the leading contribution to the AHE stems entirely from the light-hole species. Besides, the magnitude of the AHE for the holes and for the electrons appears to be comparable despite the itinerant SOC of the Γ_8^v states.

A skew scattering for a heavy-hole state is also possible but it emerges in a higher order in k. In particular, we considered a 14-band $\boldsymbol{k}\cdot\boldsymbol{p}$ model and took into account the admixture of p-like (X', Y', Z') conduction band states $\Gamma_{7,8}^c$ The corresponding wave functions are summarized in the Supplemental Material [48]. We take into account only $Q = (i\hbar/m)\langle X'|\hat{p}_y|Z\rangle$, E_0', and Δ parameters (see Fig. 2) and neglect Δ^- as the latter appears to give no contribution to the asymmetric scattering rates:

$$W^{(1)}_{lh+,lh+} = W^{(1)}_{lh-,lh-} = W^{(1)}_{lh+,lh-} = u_0^2\left[\frac{2}{9}\pi^2\left(\frac{P}{E_0}\right)^2\langle\nu\rangle k_{lh}^2(\alpha_{ex}+10\beta_{ex})J + \frac{\langle\nu\rangle}{135}\pi^2\left(\frac{Q}{E_0'+\Delta}\right)^2 k_{lh}^2(2\beta_{ex}-\gamma_{ex})J + \frac{2}{27}\pi^2\left(\frac{Q}{E_0'}\right)^2\langle\nu\rangle k_{lh}^2(10\beta_{ex}+\gamma_{ex})J\right](Y_x'Y_y - Y_y'Y_x), \tag{36}$$

$$W^{(1)}_{lh+,hh+} = W^{(1)}_{lh-,hh-} = W^{(1)}_{lh+,hh-} = W^{(1)}_{lh-,hh+} = u_0^2\left[\frac{\langle\nu\rangle}{15}\pi^2\left(\frac{Q}{E_0'+\Delta}\right)^2 k_{hh}k_{lh}(2\beta_{ex}-\gamma_{ex})J\right](Y_x'Y_y - Y_y'Y_x), \tag{37}$$

$$W^{(1)}_{hh+,hh+} = W^{(1)}_{hh-,hh-} = W^{(1)}_{hh+,hh-} = u_0^2\left[\frac{3}{5}\pi^2\left(\frac{Q}{E_0'+\Delta}\right)^2\langle\nu\rangle k_{hh}^2(2\beta_{ex}-\gamma_{ex})J\right](Y_x'Y_y - Y_y'Y_x). \tag{38}$$

The magnetic component of the scattering potential eventually gives rise to the Hall current, which would be otherwise zero in the case of nonmagnetic scatterers. Also, the matrix element $\gamma_{ex} = \langle X'|\hat{J}_{ex}|X'\rangle$ of the exchange interaction for the higher conductance band appears in the expression for the symmetrical rates. Thus, the admixture of the conduction band states to the valence band states is an important factor behind the formation of AHE driven by holes in zinc-blende semiconductors.

We would like to propose that the discovered suppression of the skew scattering of the heavy holes on nonmagnetic centers is likely to contribute to the known superlinear transverse vs longitudinal resistance scaling in p-type (Ga,Mn)As [36,43].

IV. QUANTUM WELLS

In this section we turn to low-dimensional systems and investigate the skew-scattering features for the degenerate electron gas in a quantum well (QW).

A. Rashba Hamiltonian

It is worth noting that there are different scenarios for the material SOC to affect the electron dynamics in a QW. A particularly important one is due to the so-called structure inversion asymmetry [38,44], when due to asymmetric potential profile of the QW linear in the electron momentum terms appear in the effective Rashba Hamiltonian:

$$H_R = \frac{\hbar^2 k^2}{2m} + \lambda_R(\sigma_x k_y - \sigma_y k_x). \tag{39}$$

Here m is the in-plane effective mass, and λ_R is the strength of the Rashba-type SOC. The eigen-wave-functions $\Psi_\pm = e^{i\boldsymbol{kr}}u_\pm$ corresponding to energies $\varepsilon_\pm = \hbar^2k^2/2m \pm \lambda_R k$ are given by

$$u_\pm = \frac{1}{\sqrt{2}}\begin{pmatrix}\pm i e^{-i\varphi}\\ 1\end{pmatrix}. \tag{40}$$

We note that in this model electrons exhibit strong spin-momentum locking; i.e., the orientation of $\boldsymbol{S}_k = \pm(\boldsymbol{e}_z \times \boldsymbol{k})/2$ is determined by $\boldsymbol{k}$.

Spin transport in systems with the Rashba term is being intensively studied [6,7,45]. It is now established that the skew-scattering induced AHE can behave differently depending on multiple factors. In particular, for the Rashba ferromagnet model, when in addition to Eq. (39) a magnetic Zeeman spin splitting is taken into account, the skew scattering depends crucially on the position of the Fermi energy. When both spin subbands are partially populated the third-order contributions to the asymmetric scattering rates from Eq. (4) vanish [16,18,46] and one has to go in higher orders of the Born approximation [17,37]. For a single spin subband at the Fermi energy the skew scattering is typically preserved in the third order [13]. On the contrary, considering a nonmagnetic system (meaning when no Zeeman spin splitting is taken into account) the skew scattering due to a scalar impurity does not appear at all. However, as we demonstrate below, the absence of skew scattering in 2D for this simplified model does not have a universal character and its properties can be strongly modified by various microscopic factors.

For instance, in full analogy with Γ_8^v states considered in Sec. III B, the electrons described by H_R scatter asymmetrically if the scatterer potential has an exchange part due to the impurity spin. Indeed, let us consider a short-range scattering potential of the form

$$\hat{V} = (u_0 + u_X J\hat{\sigma}_z)\delta(\boldsymbol{r}); \tag{41}$$

here u_0 and u_X correspond to the electrostatic and exchange interaction, respectively. Using the eigenstates from Eq. (40) we get the following expression for the skew-scattering rates:

$$B = \pi u_X \left(u_0^2 - u_X^2 J^2\right)\langle\nu\rangle \begin{pmatrix} \nu_+ & -\nu_- \\ -\nu_+ & \nu_- \end{pmatrix}, \tag{42}$$

where $\langle\nu\rangle = (\nu_+ + \nu_-)/2$ is an average DOS at the Fermi energy E, and the DOS $\nu_\pm$ in each subband is given by

$$\nu_\pm = \frac{m}{2\pi\hbar^2}\left[1 \mp \left(1 + \frac{2\hbar^2 E}{m\alpha^2}\right)^{-1/2}\right]. \tag{43}$$

Thus, we attest to the appearance of finite skew-scattering rates due to nonzero exchange interaction constant u_X.

In contrast to the the Luttinger Hamiltonian case considered above, here the asymmetry in the scattering rates does lead to the appearance of finite anomalous Hall conductivity. Indeed, let us calculate the electric current for this model. We keep to the strong SOC regime in the sense that we assume that the broadening of DOS due to electron scattering does not exceed the Rashba spin splitting $\lambda_R k_F \tau/\hbar \gg 1$. In this case the electron transport can be described using the approach of Sec. II with the unperturbed expressions for $\nu_\pm$ from Eq. (43) and exact Rashba spectrum from Eq. (39). Calculating the longitudinal part of the collision integral using the eigenstates Eq. (40) we obtain

$$A = \begin{pmatrix} -\tau_R^{-1} + \gamma_+ & -\gamma_- \\ -\gamma_+ & -\tau_R^{-1} + \gamma_- \end{pmatrix},$$
$$\tau_R^{-1} \approx \frac{2\pi}{\hbar} n_i u_0^2 \langle\nu\rangle, \quad \gamma_\pm = \frac{2\pi}{\hbar} n_i \frac{u_0^2}{4}\nu_\pm; \tag{44}$$

here the parameters τ_R^{-1}, $\gamma_\pm$ are given in the leading order with respect to u_X/u_0. Using Eqs. (14) and (15) we calculate the Hall current,

$$j_y = e^2 E_x 2\pi v_F^2 \tau_R u_X J(\nu_+ - \nu_-)^2. \tag{45}$$

Therefore, in the presence of magnetic scatterers the transverse current is not canceled out restoring AHE for the 2D Rashba-type Hamiltonian. It is important to emphasize that apart from the exchange interaction strength the Hall current is also proportional to the difference in DOS for the two subbands $\nu_+ - \nu_-$ at the Fermi level. The strong SOC regime assumed in this calculation ensures $\nu_+ \neq \nu_-$; otherwise the disorder-induced smearing of the DOS would eliminate the spin-dependent part $\nu_+ \approx \nu_-$ leading to the vanishing of the Hall current.

B. Size-quantization effects

Let us consider another microscopic scenario capable of restoring the significance of the skew scattering in semiconductor QW systems. Besides the Rashba Hamiltonian model, the SOC can be explicitly inherited by QW conductive band electrons from the bulk band structure considered in detail in Sec. III B. Indeed, considering the size-quantization effect along the QW growth axis of electron states given by Eq. (19) one can derive [47] the following expressions for the electron wave functions in a QW:

$$\Psi_{s,\boldsymbol{k}}(\boldsymbol{r}) = c_k e^{i\boldsymbol{k}\cdot\boldsymbol{r}}[u_s(z)\cdot S + \boldsymbol{v}_{s\boldsymbol{k}}(z)\cdot \boldsymbol{R}], \tag{46}$$

$$\boldsymbol{v}_{s\boldsymbol{k}} = i(\mathcal{A}\boldsymbol{K} - i\mathcal{B}\boldsymbol{\sigma}\times\boldsymbol{K})u_s(z), \tag{47}$$

where $\boldsymbol{K} = (\boldsymbol{k}, -i\partial_z)$ and $u_s(z) = \varphi(z)|s\rangle$ contains an envelope wave function reflecting the size quantization $\varphi(z)$. The dominant part of the matrix element of the scattering potential $u_0(\boldsymbol{r})$ calculated using the wave functions from above can be expressed as [47]

$$V_{kk'} = V_0\{1 + a\boldsymbol{\sigma}[(\boldsymbol{k}+\boldsymbol{k}')\times\boldsymbol{e}_z]\},$$
$$a = (2\mathcal{A}\mathcal{B} + \mathcal{B}^2)\int u_0\varphi^*(z)\frac{\partial}{\partial z}\varphi(z), \tag{48}$$

where $a = (2\mathcal{A}\mathcal{B} + \mathcal{B}^2)\langle\varphi|u_0\partial_z|\varphi\rangle_z$; here the average goes over the QW growth axis z. Using this matrix element we calculate the skew-scattering rates from Eq. (4),

$$W_{kk'}^{ss'} = 2\pi\nu V_0^3 a^2 \sigma_z^{ss'}(\boldsymbol{k}\times\boldsymbol{k}')_z. \tag{49}$$

In fact, the obtained expression mimics the skew-scattering rates of the Γ_6^c electron in bulk but the coefficient a now contains information on the QW size quantization. In particular, when impurities do not possess an additional magnetic moment (hence no exchange interaction part), the emergence of skew scattering visible from Eq. (49) is already sufficient to give rise to nonzero spin Hall conductivity. Indeed, performing the standard procedure according to Eq. (14) we arrive at the following expression for the Hall current j_H^s for electrons with spin projection s:

$$j_H^s = -\frac{e^2 E_x \hbar\nu v}{n_i V_0}(k_F a)^2. \tag{50}$$

The nonvanishing spin Hall current can be converted into the electric transverse signal upon nonequilibrium carrier spin polarization.

The presented analysis reveals that in the 2D case the skew scattering is not universally suppressed but rather depends on the microscopic details of the SOC-induced conduction band states and the scatterer structure. Moreover, for the Rashba SOC the skew scattering emerges when an impurity possesses a magnetic moment.

V. SUMMARY

We have clarified the important differences in microscopic mechanisms and emergent features of the skew scattering of conductance band electrons and valence band holes on nonmagnetic and paramagnetic centers in zinc-blende semiconductors. As we have demonstrated the effect of SOC on the band structure and the skew scattering are not directly related although based on the same physics of SOC. In particular, for a bulk semiconductor the skew scattering is determined by the wave function properties. While SOC leads to a rather large splitting of the spectra for the valence band, the skew scattering is suppressed for the heavy holes. For the light holes it is of a similar magnitude as for the conduction band electrons subject to $\boldsymbol{k}\cdot\boldsymbol{p}$ driven coupling between the bands. We also demonstrated that presence of a magnetic impurity qualitatively modifies the skew-scattering properties. Most brightly it is seen for the 3D holes and 2D Rashba electrons. In these cases the scattering on a magnetic center allows for the asymmetry leading to the extrinsic contribution to the anomalous Hall effect otherwise suppressed. The exchange interaction between the magnetic moment of the scatterer and the incident carrier spin leads to the spin-independent scattering asymmetry, hence, to the anomalous Hall effect even in the absence of the spin polarization of the mobile carriers.

Our findings enrich the understanding of the spin-dependent transport and motivate further experimental probes of the revealed intricate properties of the skew scattering in semiconductors.

Further calculation details and intermediate formulas are given in the Supplemental Material [48].

ACKNOWLEDGMENTS

I.V.R. and E.L. acknowledge Academy of Finland (Grant No. 318500), I.V.R. is grateful to Weizmann Institute of Science for support and hospitality. We are grateful to N. S. Averkiev and A. H. MacDonald for valuable discussions.

[1] B. T. Zhou, K. Taguchi, Y. Kawaguchi, Y. Tanaka, and K. T. Law, Spin-orbit coupling induced valley Hall effects in transition-metal dichalcogenides, Commun. Phys. **2**, 26 (2019).

[2] M. Onga, Y. Zhang, T. Ideue, and Y. Iwasa, Exciton Hall effect in monolayer MoS_2, Nat. Mater. **16**, 1193 (2017).

[3] C. Song, R. Zhang, L. Liao, Y. Zhou, X. Zhou, R. Chen, Y. You, X. Chen, and F. Pan, Spin-orbit torques: Materials, mechanisms, performances, and potential applications, Prog. Mater. Sci. **118**, 100761 (2020).

[4] A. Manchon, J. Železný, I. M. Miron, T. Jungwirth, J. Sinova, A. Thiaville, K. Garello, and P. Gambardella, Current-induced spin-orbit torques in ferromagnetic and antiferromagnetic systems, Rev. Mod. Phys. **91**, 035004 (2019).

[5] A. Soumyanarayanan, N. Reyren, A. Fert, and C. Panagopoulos, Emergent phenomena induced by spin-orbit coupling at surfaces and interfaces, Nature (London) **539**, 509 (2016).

[6] N. Nagaosa, J. Sinova, S. Onoda, A. H. MacDonald, and N. P. Ong, Anomalous Hall effect, Rev. Mod. Phys. **82**, 1539 (2010).

[7] J. Sinova, S. O. Valenzuela, J. Wunderlich, C. H. Back, and T. Jungwirth, Spin Hall effects, Rev. Mod. Phys. **87**, 1213 (2015).

[8] J. Smit, The spontaneous Hall effect in ferromagnetics I, Physica **21**, 877 (1955).

[9] J. Smit, The spontaneous Hall effect in ferromagnetics II, Physica **24**, 39 (1958).

[10] A. Fert and O. Jaoul, Left-Right Asymmetry in the Scattering of Electrons by Magnetic Impurities, and a Hall Effect, Phys. Rev. Lett. **28**, 303 (1972).

[11] A. Fert and A. Friederich, Skew scattering by rare-earth impurities in silver, gold, and aluminum, Phys. Rev. B **13**, 397 (1976).

[12] A. Fert, A. Friederich, and A. Hamzic, Hall effect in dilute magnetic alloys, J. Magn. Magn. Mater. **24**, 231 (1981).

[13] N. A. Sinitsyn, A. H. MacDonald, T. Jungwirth, V. K. Dugaev, and J. Sinova, Anomalous Hall effect in a two-dimensional Dirac band: The link between the Kubo-Streda formula and the semiclassical Boltzmann equation approach, Phys. Rev. B **75**, 045315 (2007).

[14] V. N. Abakumov and I. N. Yassievich, Anomalous Hall effect for polarized electrons in semiconductors, Sov. Phys. JETP **34**, 1375 (1972).

[15] M. I. Dyakonov and V. I. Perel, Current-induced spin orientation of electrons in semiconductors, Phys. Lett. A **35**, 459 (1971).

[16] M. Borunda, T. S. Nunner, T. Lück, N. A. Sinitsyn, C. Timm, J. Wunderlich, T. Jungwirth, A. H. MacDonald, and J. Sinova, Absence of Skew Scattering in Two-Dimensional Systems: Testing the Origins of the Anomalous Hall Effect, Phys. Rev. Lett. **99**, 066604 (2007).

[17] A. A. Kovalev, K. Výborný, and J. Sinova, Hybrid skew scattering regime of the anomalous Hall effect in Rashba systems: Unifying Keldysh, Boltzmann, and Kubo formalisms, Phys. Rev. B **78**, 041305(R) (2008).

[18] N. A. Sinitsyn, Semiclassical theories of the anomalous Hall effect, J. Phys.: Condens. Matter **20**, 023201 (2008).

[19] B. Zimmermann, K. Chadova, D. Ködderitzsch, S. Blügel, H. Ebert, D. V. Fedorov, N. H. Long, P. Mavropoulos, I. Mertig, Y. Mokrousov, and M. Gradhand, Skew scattering in dilute ferromagnetic alloys, Phys. Rev. B **90**, 220403(R) (2014).

[20] B. Zimmermann, N. H. Long, P. Mavropoulos, S. Blügel, and Y. Mokrousov, Influence of complex disorder on skew-scattering Hall effects in $L1_0$-ordered FePt alloy, Phys. Rev. B **94**, 060406(R) (2016).

[21] A. Hönemann, C. Herschbach, D. V. Fedorov, M. Gradhand, and I. Mertig, Absence of strong skew scattering in crystals with multi-sheeted Fermi surfaces, J. Phys.: Condens. Matter **31**, 085803 (2019).

[22] G.-Y. Guo, S. Maekawa, and N. Nagaosa, Enhanced Spin Hall Effect by Resonant Skew Scattering in the Orbital-Dependent Kondo Effect, Phys. Rev. Lett. **102**, 036401 (2009).

[23] D. Maryenko, A. Mishchenko, M. Bahramy, A. Ernst, J. Falson, Y. Kozuka, A. Tsukazaki, N. Nagaosa, and M. Kawasaki, Observation of anomalous Hall effect in a non-magnetic two-dimensional electron system, Nat. Commun. **8**, 14777 (2017).

[24] J. Kondo, Anomalous Hall effect and magnetoresistance of ferromagnetic metals, Prog. Theor. Phys. **27**, 772 (1962).

[25] M. A. Rakitskii, K. S. Denisov, I. V. Rozhansky, and N. S. Averkiev, Fingerprints of the electron skew scattering on paramagnetic impurities in semiconductor systems, Appl. Phys. Lett. **118**, 032105 (2021).

[26] I. A. Ado, I. A. Dmitriev, P. M. Ostrovsky, and M. Titov, Anomalous Hall Effect in a 2D Rashba Ferromagnet, Phys. Rev. Lett. **117**, 046601 (2016).

[27] S. Onoda, N. Sugimoto, and N. Nagaosa, Intrinsic versus Extrinsic Anomalous Hall Effect in Ferromagnets, Phys. Rev. Lett. **97**, 126602 (2006).

[28] T. Jungwirth, Q. Niu, and A. H. MacDonald, Anomalous Hall Effect in Ferromagnetic Semiconductors, Phys. Rev. Lett. **88**, 207208 (2002).

[29] S. Y. Liu, N. J. M. Horing, and X. L. Lei, Long-range scattering effects on spin Hall current in *p*-type bulk semiconductors, Phys. Rev. B **73**, 205207 (2006).

[30] P. Kleinert and V. Bryksin, Theory of spin-Hall transport of heavy holes in semiconductor quantum wells, J. Phys.: Condens. Matter **18**, 7497 (2006).
[31] W. Zhi-Gang and Z. Ping, Anomalous Hall effect of heavy holes in III-V semiconductor quantum wells, Chin. Phys. **16**, 517 (2007).
[32] J. Sinova, T. Jungwirth, J. Kučera, and A. H. MacDonald, Infrared magneto-optical properties of (III,Mn)V ferromagnetic semiconductors, Phys. Rev. B **67**, 235203 (2003).
[33] A. A. Kovalev, J. Sinova, and Y. Tserkovnyak, Anomalous Hall Effect in Disordered Multiband Metals, Phys. Rev. Lett. **105**, 036601 (2010).
[34] S. H. Chun, Y. S. Kim, H. K. Choi, I. T. Jeong, W. O. Lee, K. S. Suh, Y. S. Oh, K. H. Kim, Z. G. Khim, J. C. Woo, and Y. D. Park, Interplay between Carrier and Impurity Concentrations in Annealed $Ga_{1-x}Mn_xAs$: Intrinsic Anomalous Hall Effect, Phys. Rev. Lett. **98**, 026601 (2007).
[35] L. N. Oveshnikov, V. A. Kulbachinskii, A. B. Davydov, B. A. Aronzon, I. V. Rozhansky, N. S. Averkiev, K. I. Kugel, and V. Tripathi, Berry phase mechanism of the anomalous Hall effect in a disordered two-dimensional magnetic semiconductor structure, Sci. Rep. **5**, 17158 (2015).
[36] D. Chiba, A. Werpachowska, M. Endo, Y. Nishitani, F. Matsukura, T. Dietl, and H. Ohno, Anomalous Hall Effect in Field-Effect Structures of (Ga,Mn)As, Phys. Rev. Lett. **104**, 106601 (2010).
[37] A. A. Kovalev, Y. Tserkovnyak, K. Výborný, and J. Sinova, Transport theory for disordered multiple-band systems: Anomalous Hall effect and anisotropic magnetoresistance, Phys. Rev. B **79**, 195129 (2009).
[38] R. Winkler, *Spin-Orbit Coupling Effects in Two-Dimensional Electron and Hole Systems*, Springer Tracts in Modern Physics (Springer, Berlin, 2003).
[39] E. L. Ivchenko and G. E. Pikus, *Superlattices and Other Heterostructures: Symmetry and Optical Phenomena* (Springer, Berlin, Heidelberg, 1997).
[40] M. Foygel and A. G. Petukhov, Scattering by atomic spins and magnetoresistance in dilute magnetic semiconductors, Phys. Rev. B **76**, 205202 (2007).
[41] S. D. Ganichev, S. A. Tarasenko, V. V. Bel'kov, P. Olbrich, W. Eder, D. R. Yakovlev, V. Kolkovsky, W. Zaleszczyk, G. Karczewski, T. Wojtowicz, and D. Weiss, Spin Currents in Diluted Magnetic Semiconductors, Phys. Rev. Lett. **102**, 156602 (2009).
[42] J. Schliemann, Theoretical study of interacting hole gas in *p*-doped bulk III-V semiconductors, Phys. Rev. B **74**, 045214 (2006).
[43] M. Glunk, J. Daeubler, W. Schoch, R. Sauer, and W. Limmer, Scaling relation of the anomalous Hall effect in (Ga,Mn)As, Phys. Rev. B **80**, 125204 (2009).
[44] Y. A. Bychkov and É. I. Rashba, Properties of a 2D electron gas with lifted spectral degeneracy, JETP Lett. **39**, 78 (1984).
[45] A. Manchon, H. Koo, J. Nitta, S. Frolov, and R. Duine, New perspectives for Rashba spin-orbit coupling, Nat. Mater. **14**, 871 (2015).
[46] T. S. Nunner, N. A. Sinitsyn, M. F. Borunda, V. K. Dugaev, A. A. Kovalev, A. Abanov, C. Timm, T. Jungwirth, J.-i. Inoue, A. H. MacDonald, and J. Sinova, Anomalous Hall effect in a two-dimensional electron gas, Phys. Rev. B **76**, 235312 (2007).
[47] N. Averkiev, L. Golub, and M. Willander, Spin relaxation anisotropy in two-dimensional semiconductor systems, J. Phys.: Condens. Matter **14**, R271 (2002).
[48] See Supplemental Material at http://link.aps.org/supplemental/10.1103/PhysRevB.106.085203 for calculation details and intermediate formulas.